Wirelessly powered and remotely controlled valve-array for highly multiplexed analytical assay automation on a centrifugal microfluidic platform

Saraí M. Torres Delgado[a,c], David J. Kinahan[b,*], Lourdes Albina Nirupa Julius[b], Adam Mallette[b,1], David Sáenz Ardila[a], Rohit Mishra[b], Celina M. Miyazaki[b,2], Jan G. Korvink[c], Jens Ducrée[b], Dario Mager[c]

[a]*Laboratory for Simulation, Department of Microsystems Engineering (IMTEK), University of Freiburg, Georges-Koehler-Allee 103, Freiburg im Breisgau 79110, Germany.*
[b]*FPC@DCU - Fraunhofer Project Center for Embedded Bioanalytical Systems at Dublin City University, Glasnevin, Dublin 9, Ireland.*
[c]*Institute of Microstructure Technology, Karlsruhe Institute of Technology, Hermann-von-Helmholtz-Platz 1, Eggenstein-Leopoldshafen 76344, Germany.*

Abstract

In this paper we present a wirelessly powered array of 128 centrifugo-pneumatic valves that can be thermally actuated on demand during spinning. The valves can either be triggered by a predefined protocol, wireless signal transmission via Bluetooth, or in response to a sensor monitoring parameters like temperature or homogeneity of the dispersion. Upon activation of a resistive heater, a low-melting membrane (Parafilm^{TM}) is removed to vent an entrapped gas pocket, thus letting the incoming liquid wet an intermediate dissolvable film and thus open the valve. The proposed system allows up to 12 heaters to be activated in parallel with a response time below 3 seconds, potentially, resulting in 128 actuated valves in under 30 seconds. We demonstrate with three examples of common and standard procedures how the proposed technology could become a powerful tool for implementing diagnostic assays on Lab-on-a-Disc. First, we implement wireless actuation of 64 valves during rotation in a freely programmable sequence, or upon user input in real time. Then, we show a closed-loop centrifugal flow control sequence where the state of mixing between reagents evaluated from stroboscopically recorded images triggers the opening of valves. In our last experiment valving and closed-loop control are used to facilitate centrifugal processing of whole blood.

Keywords: Wireless actuation, centrifugo-pneumatic valves, Lab-on-a-Disc, centrifugal platform, automation, closed-loop control

1. Introduction

Increasingly over the past decade, centrifugal microfluidic systems (Ducrée et al., 2007; Madou et al., 2006; Strohmeier et al., 2015; Smith et al., 2016) have been developed for a variety of application fields such as biomedical diagnostics (Gorkin et al., 2010; Tang et al., 2016) and environmental monitoring (Smith et al., 2016; Kong and Salin, 2012; Hwang et al., 2013; Czugala et al., 2012). The cartridges, which have dimensions akin to commonly available optical data media such as CDs or DVDs, are typically rotated by a versatile and compact instrument featuring a conventional spindle motor. A major advantage of this Lab-on-a-Disc (LoaD) platform is their inherent capability to centrifuge samples, extremely useful for Laboratory Unit Operations (LUOs) (Strohmeier et al., 2015) for blood processing (Kinahan et al., 2014b, 2016b) and particle / cell handling (Glynn et al., 2013; Burger et al., 2012). These LoaD devices can be designed to process and analyse the sample in a fully automated fashion, thus making them particularly useful for decentralised testing, e.g., in point-of-care scenarios (Smith et al., 2016).

However, as all liquids on-disc are simultaneously subjected to the centrifugal field, flow control elements, such as valves, have become fundamental enabling technologies for coordinating sample preparation steps

* Corresponding author: david.kinahan@dcu.ie
[1]Department of Chemical and Biomolecular Engineering, University of Notre Dame, Notre Dame, IN, United States.
[2]Science and Technology Centre for Sustainability, Federal University of São Carlos, Campus Sorocaba, SP - Brazil.

such as mixing, metering, reagent release and other LUOs. Valving on the centrifugal platform can be categorised into active (externally actuated) and passive (rotationally controlled) schemes.

Passive valves switch upon changing the spin rate. This type of valve is based on unbalancing the hydrostatic equilibrium between rotationally induced hydrostatic pressure and the other forces acting on liquid elements such as pneumatic (counter) pressure or capillary force; thus, the key advantage is that the only control input required is modulating the spin-rate of the system innate spindle motor. The high-pass version of this valving type yields upon exceeding a certain rotational frequency; these include capillary burst valves (Chen et al., 2008; Moore et al., 2011; Thio et al., 2013; Li et al., 2010; Haeberle et al., 2006), centrifugo-pneumatic dissolvable film valves (Gorkin III et al., 2012; Nwankire et al., 2014, 2015; Mishra et al., 2015), burstable foils (van Oordt et al., 2013), elastomeric membranes (Hwang et al., 2011) and dead-end pneumatic chambers (Mark et al., 2011). On the other hand, low-pass valves open upon a reduction of the rotational frequency. These flow control elements include conventional (hydrophilic) siphons (Siegrist et al., 2010; Kitsara et al., 2014) and pneumatically enhanced centrifugo-pneumatic siphon valves (Gorkin III et al., 2010; Godino et al., 2013; Schwemmer et al., 2015). Recently, Kinahan et al. (2014a, 2015, 2016c) introduced event-triggered valves, whereby liquid arriving at strategically chosen points on the disc dissolves a film and, by venting an interconnected pneumatic chamber, triggers the release of liquid from a distal reservoir. For further details on these valving technologies, the reader can refer to the cited literature.

Platforms enabled by active valves typically offer greater levels of integration density compared with the rotationally actuated valves, but at the expense of increased cost and complexity. However, the decreasing cost, improved ease-of-use and availability of micro-components has resulted in increasing popularity of such valving schemes. Externally actuated valves can broadly be characterised as those for which a peripheral instrument (other than the platform-innate spindle motor) transfers energy to the disc.

The range of interaction methods that have been implemented include, connection to external pressure sources, such as an external dry compressed air tank connected through an outlet tube (Kong and Salin, 2010, 2012), or in a more elegant way as reported by Clime et al. (2015), with the integration of regulated and programmable electromechanical pumps and valves.

A second method is to induce phase changes in plugs made of paraffin wax (Abi-Samra et al., 2011; Al-Faqheri et al., 2013; Zainal et al., 2017), ferrowax (Lee et al., 2011; Park et al., 2007) or thin polymer films (Garcia-Cordero et al., 2010). These materials are used as physical barriers and their phase transition is used to open or close a channel when radiating thermal energy directly onto them. Radiation sources include a solid-state laser (Garcia-Cordero et al., 2010; Lee et al., 2011; Park et al., 2007), a pair of electromagnetically coupled RF resonators (Zainal et al., 2017) where the receiver coil acts as a heater, a focused halogen lamp (Abi-Samra et al., 2011), or even by positioning a hot-air gun closely to the surface of the microfluidics disc (Al-Faqheri et al., 2013). There is also the possibility of freezing a small amount of the liquid creating a tight seal, known as ice-valves (Amasia et al., 2012).

A third method is to integrate external electromechanical devices to exert a force over the disc. For example, in (Carpentras et al., 2015; Kinahan et al., 2016a; Kim et al., 2016; Cai et al., 2015) components such as magnets (Carpentras et al., 2015), screw-like elements (Kim et al., 2016), a blade (Kinahan et al., 2016a), or even a spring plunger (Cai et al., 2015) were incorporated to the centrifugal platform. These components lift off movable plugs (Carpentras et al., 2015), pierce membranes (Kinahan et al., 2016a), or press against either an elastic epoxy diaphragm embedded on the disc (Kim et al., 2016), or a PDMS microchannel (Cai et al., 2015) present in it. Another method requires a secondary rotation of the chip to change the relative direction of the centrifugal field (Kawai et al., 2013; Geissler et al., 2015; Miao et al., 2015; Zhu et al., 2017; Wang et al., 2013).

Full integration of active valving on-disc requires not only the valving method but the inclusion of a wirelessly powered system (Zhu et al., 2017; Loo et al., 2017; Torres Delgado et al., 2016a; Höfflin et al., 2015; Torres Delgado et al., 2016b). Therefore, we combine the previously introduced 'electrified Lab-on-a-Disc' (eLoaD) platform (Torres Delgado et al., 2016a,b) with the dissolvable film valves introduced in (Kinahan et al., 2014a, 2015, 2016c) and an array of resistive heaters to produce a platform which can actuate up to 128 valves in a time and rotation speed -independent sequence. The platform can be controlled using two methods. In the first, an internal script preloaded in the platform can automatically execute a defined and accurately timed sequence of valve actuation. The second method allows arbitrary actuation and relies on sending commands over Bluetooth to the controller.

To demonstrate the capabilities of this wirelessly powered platform and exemplify how it could become a

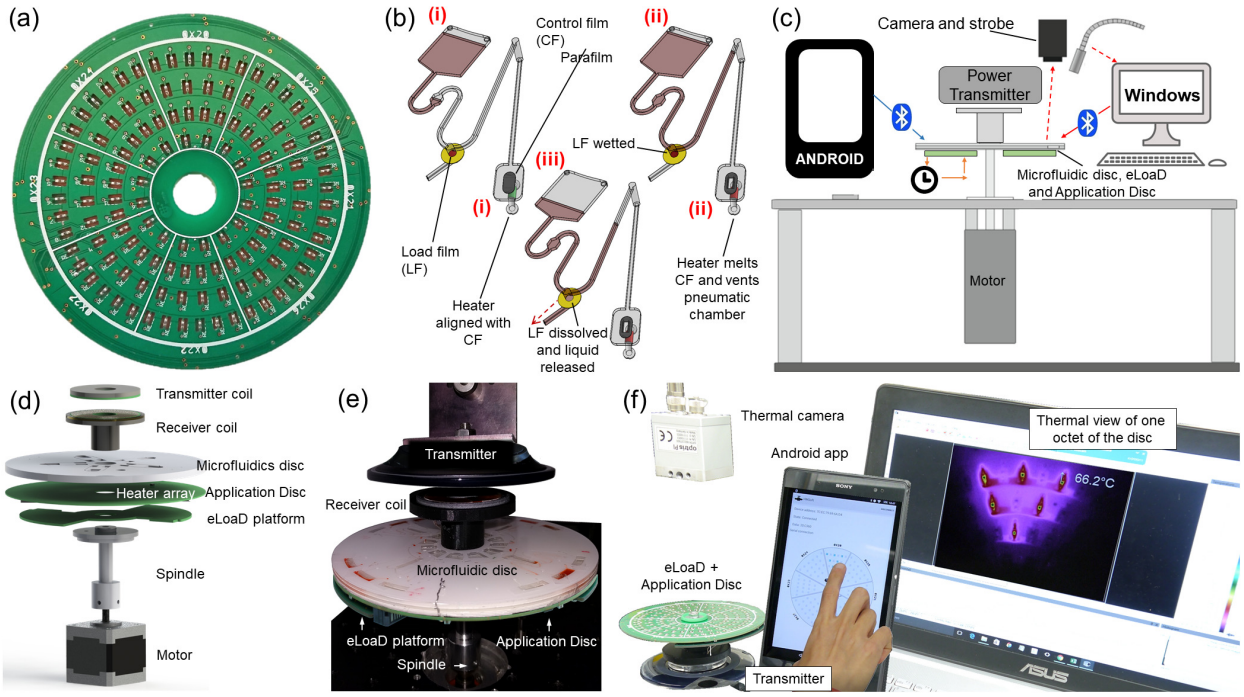

Figure 1: (a) Disc featuring 128 wirelessly powered and controlled micro-heaters for independent actuation of the normally-closed valves. (b) Valve operation and (c) platform concept showing the three control options – internal timing, manual control via an Android app and closed-loop or manual control via a Windows PC. (d) Exploded view of the platform (adapted from (Torres Delgado et al., 2016a)). (e) The assembled system showing a commercial phone charger (transmitter coil) mounted above the spin-stand (f) IR thermography during testing of the system. Note the heated resistors correspond to those manually activated using the android app (See Movie-S1 available as supplementary material).

powerful tool for diagnosis experiments we include several application examples with increasing complexity. First, we use it to actuate valves in a defined sequence on a disc with 64-valves, this shows the independence of the switching sequence from physical properties like the spin rate. We then use colour based closed-loop image analysis to mix dyed water with salt water through 'shake-mode' Euler-force mixing (Kinahan et al., 2015) exposing in this way, the capability to trigger the valves based on measurement results from the disc. Finally, for the last experiment, both, the valving and closed-loop control are used to facilitate a standard and one of the most common procedures used in implementing diagnostic assays on Lab-on-a-Disc, centrifugal processing of whole blood.

2. Material and methods

This section describes the design and implementation of the circuitry that in combination with the eLoaD platform (Torres Delgado et al., 2016a,b) enables the control of up to 128 resistive heaters as part of a novel active valving method. The described circuitry makes the actuation method and its full integration into the (also described) rotating platform possible. The following subsections also explain the design and fabrication method of the microfluidic discs, as well as the hardware and software necessary for the proper execution and interfacing of the experiments (See Fig. 1 and Movie-S1 available as supplementary material).

2.1. The eLoaD platform

The eLoaD platform allows continuous measurement of experimental parameters during spinning. It is conceived in a modular manner, whereby an interchangeable and non-disposable 'Application Disc' can be specifically designed and fitted to the eLoaD platform and so the system can be adapted for a range of optical, electrochemical and other sensing and actuation mechanisms (Torres Delgado et al., 2016b,a).

The platform comprises a wireless power receiver and an Arduino compatible microcontroller. The power receiver is part of the 5 W-series of the Qi Standard for wireless power transfer (WPC, 2016), more commonly used to charge smartphones. The microcontroller, based on the ATmega32U4, has 17 digital input/output

pins (0 V or 5 V), 6 of which can be used as Pulse-Width Modulation (PWM) outputs (used, for example, for regulated heating) and 12 as analogue inputs. It also integrates the necessary channels for internal communication among the microcontroller, sensors, actuators, and the user such as the Inter-Integrated Circuit (I^2C) and Serial Peripheral Interface (SPI) communication protocols. The platform also features an SD-card module for when large data acquisition is needed and a Bluetooth module for real time bidirectional communication.

As stated in (Torres Delgado et al., 2016b,a), after transmission, rectification and regulation losses, the available power to sustain the platform is at least 4 W. The end user can then select the modules needed for a specific experiment and switch off the rest. The available power for the Application Disc depends on the number of active modules. However, a minimum of 3.5 W is even guaranteed when all modules are in use.

2.2. Application Disc for thermal actuation of microfluidic valves

As mentioned before the 'Application Disc' is a second interchangeable and non-disposable printed circuit board (PCB) specifically designed to fit on the eLoaD platform, adapted to the particular applications, in this case as a valving mechanism. The Application Disc employed during our experiments (in Sec. 3) is a 12 cm-diameter disc made of a standard double-sided PCB with 2 conductor layers of 35 μm-thick copper and a 1.5 mm-thick FR4 substrate. The actual Application Disc can be seen in Fig. 1(a). This disc was fabricated using commercially available PCB manufacturing technology. Sensors and actuators are usually located on the top layer of the Application Disc in direct contact with the fluidic disc, while the rest of components of the circuitry in use (e.g. driving, control, amplification, filtering) lay on the bottom side.

The architecture of the microfluidic disc and the number of valves used will depend entirely on the protocol to be executed. Therefore, the number of resistive heaters used for that specific protocol will differ too. However, for validation and demonstration of the capabilities of the proposed valving method, a modular and multi-purpose electronic layout was developed, for which we considered both the electrical and thermal aspects.

2.2.1. Application disc' top layer: array of resistive heaters

The overall thermal resistance is mainly determined by the printed circuit board design, assembly of the platform and the environmental conditions surrounding the experiment setup. As opposed to ideal PCB design which is optimized for the electronic layout and the components' position for enhanced heat dissipation into the substrate material, our goal was to maximise heat transfer into the microfluidic disc for melting the Parafilm^{TM} layer. In Sec. 3.1, we further investigate structuring possibilities.

We chose surface-mount (SMD) resistors in a 0603 package as the heater elements because of their:

- *size and level of integration:* 0603 SMD components are extremely compact (1.6 mm by 0.8 mm), highly integrable and, if chosen and placed properly, no thermal cross-talk between an active heater and neighbour Parafilm^{TM}membranes occurs. This allows having a dense array of individually addressable microfluidic valve actuators implemented on a single layer of a printed circuit board.

- *high power density:* the electrical current passing through a resistor is proportional to the voltage being applied across its terminals. The electrical power dissipated by an active resistor is, also proportional to the temperature the component reaches. In this case we applied 5 V to 100 Ω resistors, resulting in 250 mW being consumed by each resistor.

- *response time:* as discussed in detail in Sec. 3.1, within a few seconds a resistor can reach temperatures of about 100 °C.

- *modularity:* very simple circuitry is needed to activate the resistors, because the actuation relies solely on digital (ON-OFF) signals.

Given that the available power on the platform is limited, there is a trade-off among the size of the heaters, the temperature that they can reach, and the power density of these. We performed several tests (not shown here) to carefully evaluate these characteristics, and finally selected 100 Ω SMD resistors with an encapsulation type 0603. The length and width of the resistors are 1.6 mm and 0.8 mm, respectively. The top side of the Application Disc (shown in Fig. 1(a)) fits an array of 128 of these resistors arranged in concentric circular patterns.

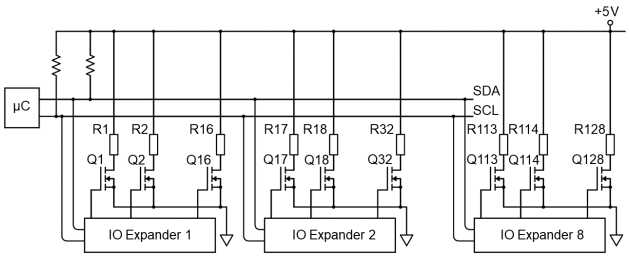

Figure 2: Schematic of the Application Disc's driving circuitry. The microcontroller (μC) is connected to eight port expanders (IO Expander x) resulting in 128 individually controllable outputs. Each output is then connected in series with an N-type MOSFET (Qx) that provides the resistive heater (Rx) with the electrical power needed to melt the Parafilm.

2.2.2. Application disc' bottom layer: driving circuitry

The bottom side of the Application Disc has the needed circuitry to individually drive each resistor. Fig. 2 shows a schematic of the driving circuitry. Since the microcontroller has a limited number of digital outputs, we used the I^2C communication protocol that allows for several components, in this case eight expanders (IO Expander 1 to 8)(PCF8575 from Texas Instruments) to be connected to the microcontroller (μC) using only two communication lines (SDA and SCL). These eight expanders with 16 outputs each, made a total of 128 individually controllable digital outputs. Since the maximum current of each 5 V output of the expanders is only 25 mA, identical to the microcontroller's outputs, the resistors (R 1 to 128) of 100 Ω cannot be connected directly (5 V/100 Ω = 50 mA). Instead, each output of an expander is connected to switch an N-type MOSFET (Q 1 to 128)(2N7002F from Philips Semiconductors) wired in series with the corresponding resistor, allowing the 50 mA of current to flow through it, directly from the main 5 V supply. The circuitry on the Application Disc consists then of 128 active channels, allowing to safely operate up to 12 valves in parallel according to the characterization shown in Sec. 3.1. Although the count of electronic components is high, due to their small size, they were integrated effortlessly on the Application disc.

2.3. User interface

The user can interface with the system using the SD-card or the Bluetooth modules. For example, the execution of a predefined and accurately timed valve control sequence loaded into the SD-card can be started via an external excitation, such as an external interrupt or Bluetooth signal, or simply by a predefined delay after the power transmission has started.

The eLoaD platform accommodates an HM-11 low energy Bluetooth module (BLE 4.0) which consumes only one tenth of the power needed for classic Bluetooth technology (BT 2.1), while maintaining the same range of communication at a lower energetic cost and size. This module constitutes a universal and easy to use wireless communication link between the Arduino-based eLoaD platform and Windows, iOS, and Android (4.3+) devices. For the case of Windows devices, it is possible to establish communication if the device has already a low energy Bluetooth module, or through a USB dongle in case it does not. It is fair to mention that, because the low energy Bluetooth modules are new to the market, they require more code development on both the Arduino and the operative system sides. Presentation of the necessary code and further optimisation is beyond the scope of this paper and is envisaged to be the subject of a future publication in a more focused journal.

The Bluetooth module can be used for executing either manual or automatic control. 'Automatic control' refers to a defined sequence execution, but now transmitted during the experiment from an external device (smartphone, tablet or a PC). Automatic control can happen in response to a set of time-dependent triggering signals or as a result of a change in the state of variable that is being monitored (e.g. mixing or sedimentation state or sample temperature). 'Manual control' requires the user to decide which valve to open and when during spinning (See Fig. 1(f) and Movie-S1 available as supplementary material). We programmed two user interfaces, one to be used with Android-based portable devices and another for a Windows PC running LabVIEW. On a Windows PC we were able to integrate the code needed for motor control and image analysis in LabVIEW with our user interface, therefore allowing for real time interaction and live measurements of the fluid flow in the disc, as well as closed-loop control of LUOs.

2.4. Microfluidic disc: manufacturing process

The discs used in this study were manufactured using Xurography (Bartholomeusz et al., 2005) as previously elucidated (Kinahan et al., 2014a, 2015) in a multilayer architecture, from layers of Poly(methyl methacrylate) (PMMA) and layers of Pressure Sensitive Adhesive (PSA) (Gorkin III et al., 2012; Kinahan et al., 2014a).

Microchannels were created from voids in PSA (50 μm thick) using a knife-cutter (CraftRobo Pro, Graphtec, USA), while larger reservoir structures are created by voids in the PMMA (1.5 mm thick) using a laser cutter (Epilog Zing, USA). To facilitate the Parafilm^{TM}, the layer configuration previously described (Kinahan et al., 2014a) was adapted to the one shown in Fig. 5(a).

The dissolvable films (DFs) are prepared by mounting them on PSA to improve sealing and to make them mechanically stable during assembly (Kinahan et al., 2014a, 2015). One grade of DF was used in this study; a low-cost film with an opening time, on contact with cold water, of $\sim$ 6 s and here called E-film (Barnyarns, Rippon, UK). For the discs used in the mixing and blood processing experiments from Sec. 3, the DF tabs are integrated into the disc during manufacture by placing them in voids in the DF support layer and then overlaying them with the DF cover layer. However, for the 64-valve disc an intact sheet of E-film was sandwiched between the DF cover and DF support layers and then placed across the entire disc.

Pneumatic venting channels were provided in the middle and lower microchannel layers, thus permitting routing of any valve on the disc to any thermal heater. Venting of the valves was facilitated by vertical vias located in the base layer. These valves were then sealed by a layer of Parafilm^{TM} which was adhered to the base using the PSA.

2.5. Spin stand

Images are acquired from a 'spin stand', described previously (Grumann et al., 2005a), in which a spindle motor (Festo EMME-AS-55-M-LS-TS, Esslingen, Germany) is controlled, via a CANOpen interface, using a custom LabVIEW program. A triggering output signal from the motor is used to synchronise it with a stroboscopic light source (Drelloscop 3244, Drello, Germany) and a sensitive, short-exposure time camera (Basler Ace 2040-90uc, Basler, Germany) such that images are acquired at 5 Hz (assuming the motor is rotating at or faster than 5 Hz). A frame sequence is acquired where the disc appears stationary; thus, permitting high-resolution stroboscopic observation of liquid flow about the disc.

2.6. Real-time data analysis and control methods

During testing, images are to be acquired from the Basler Ace camera using Basler Pylon software and saved to a folder on the PC hard-drive in bitmap format. A custom LabVIEW code is used to control the experiments. This code has three components parts; the Bluetooth communication module, the motor control module and the image analysis module. On startup, the code must be pointed at the folder described above. During operation, the code continuously monitors this folder and loads into memory the most recently created bitmap image. Images are typically loaded within 100 ms of creation and therefore this setup results in close to real-time monitoring of the camera output.

Next, the user defines a number of Regions of Interest (ROIs) in the acquired frames. These ROIs are each assigned a unique reference number. The user then defines a series of triggers. Four trigger conditions can be defined for the colour intensity of a ROI, i.e., if it:

- exceeds a pre-defined value for a set time period.
- decreases below a pre-defined value for a set time period.
- leaves, for a set time period, a defined intensity band.
- matches, for a set time period and within a defined band, the colour intensity of a second ROI.

A capability to weight the intensity in the ROI (based on the values of the Red, Green, Blue (RGB) channels) was included, white being the highest (all three colour values are at maximum) and black being the lowest (all three colour values are at zero) intensity. In addition, to compensate for variations in strobe intensity, a capability to normalise signals relative to another ROI was also included. However, due to the stability of the acquired images, this feature was not used.

With the system pre-configured, a script is loaded from a text file. The script is composed of a series of four command types:

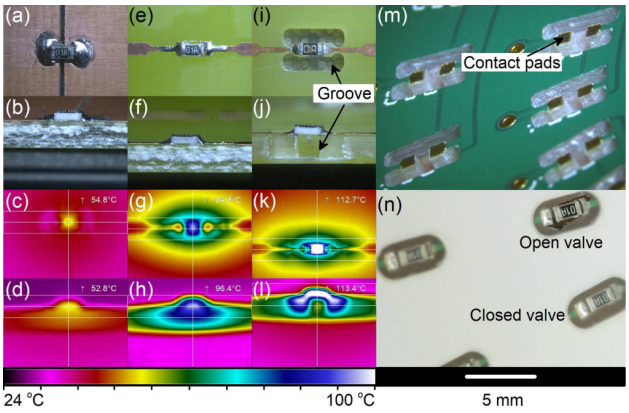

Figure 3: Thermal response of a 100 Ω SMD resistor with a package 0603 for different conductor tracks and substrate profile. (a) The resistor soldered to wide conductor tracks. (b) Side view of the resistor in (a). Infrared photograph from top (c) and side (d) views of the resistor in (a). (e) The resistor soldered to narrow conductor tracks. (f) Side view of the resistor in (e). Infrared photograph from top (g) and side (h) views of the resistor in (e). (i) The resistor over a milled groove into the FR4 substrate soldered to narrow conductor tracks. (j) Side view of the resistor in (i). Infrared photograph from top (k) and side (l) views of the resistor in (i). (m) Close-up view of the Application Disc showing in detail the grooves upon which each resistor is soldered to the shown pads. (n) Demonstration of how the resistive heaters melt the Parafilm™ (See Movie-S2 available as supplementary material).

- Motor commands and parameters including 'jog negative', 'velocity', 'acceleration' and 'stop at position'.
- Bluetooth commands which turn on and off individual heaters.
- Check trigger command has two values, the trigger number to check, and a goto waypoint. If the trigger is positive, the code proceeds to the next command. If the trigger is negative, the code steps forward or backward to the specified goto waypoint.
- Goto waypoints, each with a unique number.

Through a combination of trigger types and script commands it is possible to implement closed-loop process control with conditional decision making.

3. Experiments and results

3.1. Characterization of the system

As explained in Sec. 2.2 the PCB layout and substrate profile needs to be considered carefully to decrease heat dissipation into the substrate. Hence, three different configurations were examined. Fig. 3 shows the temperature profile from the top (Fig. 3(c), (g), and (k)) and side views (Fig. 3(d), (h), and (l)) measured with an infrared camera (PI 160, Optris GmbH, Germany) for different conducting material track widths (Fig. 3(a) and (e)) and substrate profiles (Fig. 3(i)). The localised heat dissipation on the surface of the resistor is higher when a milled groove is made into the substrate material, therefore a higher temperature can be maintained. This temperature difference is nearly 20 °C for the same electrical excitation. Therefore, Fig. 3(m) shows a close view of the Application Disc used for the experiments, which has been milled as part of the PCB manufacturing process. The milling process removed the FR4, leaving only the material needed to produce contact pads. The top side of the Application Disc shown in Fig. 1(a) has 128 resistors arranged in concentric circular patterns. For this final configuration, a temperature slew rate of ~ 17 °C/s was measured. Meaning, the resistors reach a temperature of 90 °C in ~ 4 s from room temperature (22 °C), time at which the Parafilm™ has already melted. Typically, the Parafilm™ deforms away from the heat source (see Fig. 3(n) and Movie-S2 available as supplementary material) and therefore the heater array did not require any cleaning between use.

We further measured the power available for the Application Disc with respect to an axial distance variation within the wireless power transmitter; this is shown in Fig. 4(a). This provided us with a good estimate of the distance we should maintain between the transmitter and receiver, preferably in the range from 1 mm to 5 mm. Most importantly, this curve reveals the interesting fact, that it is better to demand a certain amount

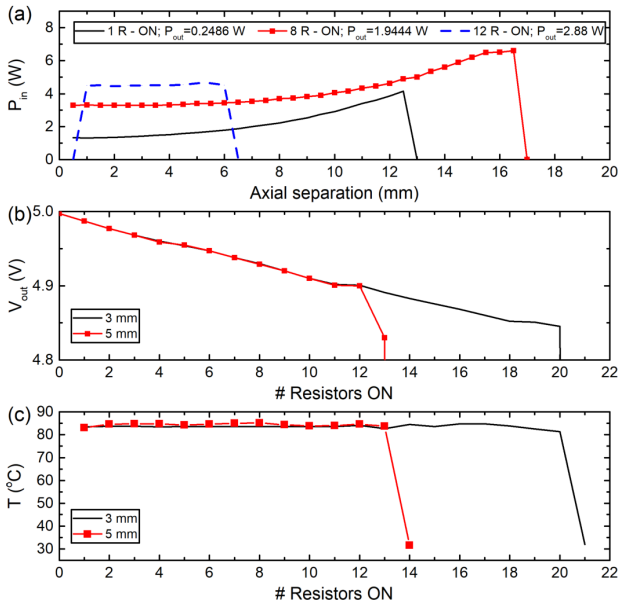

Figure 4: Application Disc's characterization: power, voltage, and temperature measurements. (a) Input power available for the Application Disc with respect to an axial distance variation from the Qi transmitter to the receiver coil (Fig. 1(d)), for three active resistor numbers. (b) Input voltage of the resistors array measured with increasing number of active resistors. (c) Surface temperature measured over one resistor with increasing number of active resistors.

of power from the system for it to be highly stable. This is demonstrated by the setup, allowing for a larger axial separation between transmitter and receiver when supplying eight resistors, rather than a single one. Fig. 4(b) shows that the output voltage diminishes only slightly while increasing the number of active resistors, until the number of resistors is sufficient to demand more power than the Qi transmitter can provide, point at which the power transmission stops. The maximum possible number of active resistors is again dependent on the distance between transmitter and receiver. The graph reveals that we can activate up to 20 resistors in parallel, consuming a total power of 4.7 W when only the microcontroller and the Bluetooth modules are active. Fig. 4(c) shows that, despite the small variation of the output voltage, the temperature measured on one resistor remains quite constant when subsequent resistors are being activated. This temperature is sufficient to melt the Parafilm^{TM} as shown in Movie-S2 (available as supplementary material). The circuitry on the Application Disc consists then of 128 active channels, allowing to safely operate up to 12 valves in parallel, for a separation distance of 5 mm. For the validation of the proposed platform, we activated a maximum of 64 valves (See next experiment).

3.2. On-demand valve actuation

The performance of the control system was first demonstrated by using the Windows PC-based control mechanism (i.e. a LabVIEW program transmitting a pre-defined sequence of Bluetooth commands). As shown in Fig. 5(b), a disc was designed which was divided in identical octets. Each octet was composed of an inner loading chamber, 8 valved aliquoting structures (3 on an inner radius and 5 on an outer radius) and an overflow chamber. Each aliquot was designed to meter $\sim$ 20 µl of dyed water (the fabrication process is described in Sec. 2.4).

This disc was first mounted on top of the Application Disc so that Parafilm^{TM} membranes (venting vias), located on the underside of the disc lined up with each heater. After placing the disc on the spin-stand, wireless power transfer was initiated. Communication was established between the on-board micro-controller and the Windows PC. Next, each octet was loaded with 180 µl of dyed water and the disc was rotated at 25 Hz. Once metering was completed the pre-programmed sequence was activated (See Movie-S3 available as supplementary material), upon application of heat (activation of each resistor), the Parafilm^{TM} quickly melts and vents the corresponding valve to atmosphere. Thus, sequential and on-demand actuation of 64-valves was demonstrated.

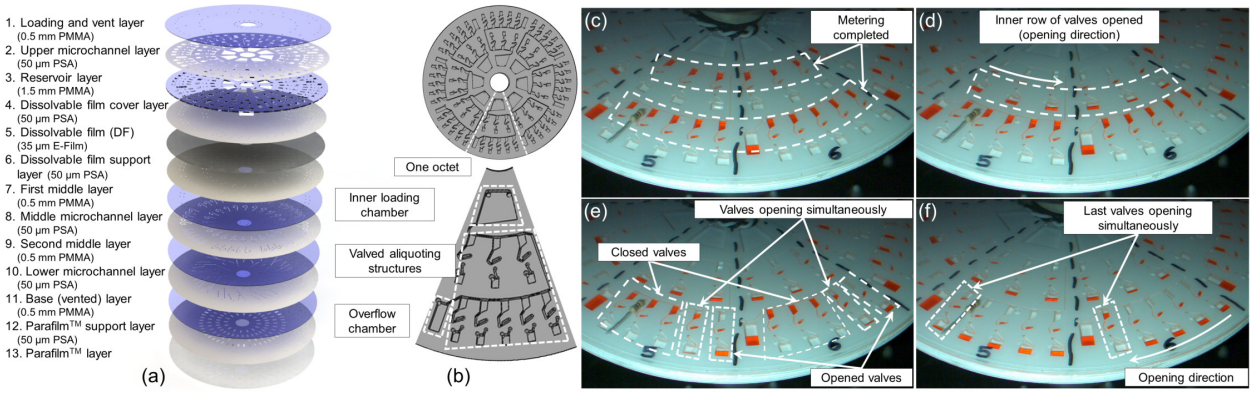

Figure 5: Disc with 64-valves. (a) Layer configuration: a ~ 4 mm multilayer architecture from layers of Poly(methyl methacrylate) (PMMA) and layers of Pressure Sensitive Adhesive (PSA) (Gorkin III et al., 2012; Kinahan et al., 2014a). The valves were sealed by a layer of Parafilm™ which was adhered to the base using the PSA. (b) Schematic representation of the disc. Each octet represents an inner loading chamber, 8 valved aliquoting structures and an overflow chamber. The actuation program, controlled by a script running in LabVIEW, from a Windows PC command actuation of valves in series. Two octets are opened in parallel before transitioning to the next two octets. The sequence opens the valves in the order they were loaded (inner row anti-clockwise and outer row clockwise) (See Movie-S3 available as supplementary material). (c) Two of the octets with metering completed. (d) The three inner valves in each octet have been opened. (e) The fifth valve in each octet opened in parallel. (f) The eight valve in each octet opened simultaneously.

3.3. Deterministic closed-loop control of fluidic mixing

In order to implement closed-loop control of on-disc processes we next apply our system to on-disc mixing. In centrifugal microfluidics, mixing is typically enhanced through the use of 'shake-mode' mixing (Grumann et al., 2005b) whereby the disc is rapidly accelerated and decelerated; thus inducing the Euler Force to agitate the liquid and enhance mixing. Here, we implement closed-loop control where we use one of the trigger modes described previously where two ROIs must match colour intensity, thereby ensuring a certain mixing result.

To present this work, we use a disc which has an approximately rectangular mixing chamber. This chamber has a valve part way down the side of the chamber, and another at the base of the chamber. We first mount the disc as described previously and load the disc with 90 µl of salt water ('Reagent' A: ~ 20 mg of salt dissolved in 1 ml of DI water) and centrifuge so that the water fills the lower half of the mixing chamber. Next, two ROIs are defined, one above the liquid level and one below the liquid level. The density difference, under centrifugal force, helps to maintain the stability of the two liquid layers. The disc is then loaded with 90 µl of dyed water ('Reagent' B: 1% concentration of common red food dye) and the test is started. As the disc is accelerated, the red dye enters the mixing chamber and is overlaid on the transparent water. As can be seen in Fig. 6(c) (at t = 0 s), and in Movie-S4 (available as supplementary material), the colour intensity of the upper ROI decreases but the colour intensity of the lower ROI stays largely steady, as red dyed water is loaded. Mass transport via diffusion starts to occur but, over the first 75 s of the test, overall mixing is negligible. When 'shake mode' is initiated, convective mixing (of reagents A and B) occurs and this is reflected in the rapid decrease in colour intensity in the lower ROI. After approximately 60 s of mixing, the colour intensities in the two ROIs converge and the pre-defined trigger condition (that the difference in intensities is less than 10 AU (arbitrary units) for 20 consecutive seconds) is met. Meeting this trigger condition results in the program leaving the mixing phase and opening the two consecutive valves in a timed sequence.

3.4. Closed-loop controlled blood processing

The last example shall be less technical and mimic a diagnostic application (using a real sample and reagents). Therefore, a closed-loop control for blood processing is implemented based on a similar approach that was previously described in (Kinahan et al., 2016b), where a siphon valve was used instead. Compared with other microfluidic systems, the centrifugal platform is highly suited to blood processing and this is a common sample preparation step in a number of assays. Here, we use density gradient media to extract both plasma and white blood cells from a whole blood sample. Initially, we extract the blood from a finger prick sample using a protocol reported previously (Glynn et al., 2014). We dilute these samples 1:1 with a

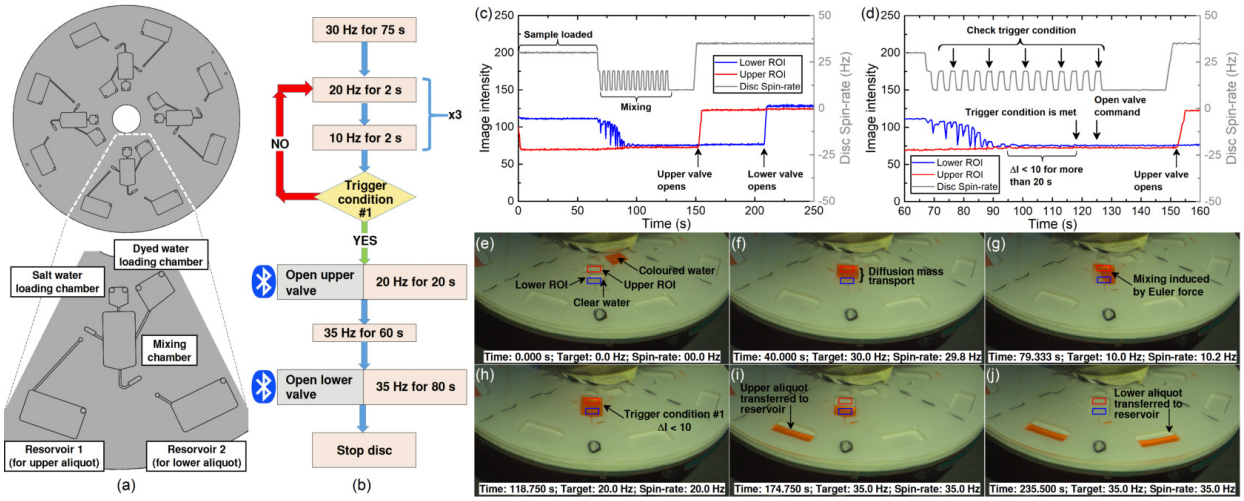

Figure 6: Closed-loop control of mixing. (a) Schematic representation of the microfluidic disc used. (b) The program decision tree. The trigger condition is the intensity (white being high and black being low) between the upper and lower regions of interest (ROIs), ΔI is less than 10 AU for 20 s (unbroken). If this condition is not met the disc undergoes another mixing cycle. If the condition is met the upper valve is opened, followed after 80 s, by the lower valve. (c) The motor spin-protocol and intensity plots for the entire experiment. Note that the colour of the intensity plots matches the ROIs shown in Fig. 6(e)-(j) (See Movie-S4 available as supplementary material). Valve opening is shown as an increase in colour intensity as the white PSA is exposed to the ROI. Note that, due to the time needed for the dissolvable film to dissolve, valve actuation is approximately 35 s after the Bluetooth command is sent to the heaters. (d) Greater detail of the system meeting Trigger Condition #1. The trigger state was found in a YES state after 5 mixing cycles. (e) The disc as coloured dye is loaded. (f) Diffusion mass transfer during the first steady-state spinning. (g) Convective mixing induced by Euler forces ('shake-mode' mixing). This convective movement is reflected in the downward spikes in the Lower ROI intensity during mixing. (h) The chamber when mixing is complete (i) upper valve opened (j) lower valve opened.

dilution buffer using a protocol also described previously (Kinahan et al., 2016b).

To process the blood, we first load 55 µl of density gradient media (Ficoll Histopaque 1077, Sigma-Aldrich) onto the disc and centrifuge at 30 Hz; this volume is chosen so that the liquid reaches the level of our inlet channel. We then load 100 µl of diluted whole blood onto the disc. The test program is then started.

The disc accelerates to 30 Hz spin-rate. This pumps the blood into the sedimentation chamber where it is overlaid on the density gradient medium (See Fig. 7 and Movie-S5 available as supplementary material). After 60 s, the program starts to monitor the colour intensity of the ROI where the red blood cells sediment. The ROI was selected at the point in the density gradient media above where, when the processing is complete, the red blood cells are expected to settle but below the peripheral blood mononuclear cell layer. Once processing is complete, the liquid at this location should be free of both white blood cells and red blood cells and so will be transparent.

In contrast to the original experiment (Kinahan et al., 2016b), the new approach allows to measure the colour composition of the analyte at different positions and trigger the valves based on the sedimentation state. When the colour intensity in this ROI increases above a certain limit (above 155 AU continuously for 20 s) the blood processing is deemed complete and the program issues a command, via Bluetooth, to open the upper valve. At this point, the program progresses to monitor the second ROI.

The second ROI monitors the colour intensity of the plasma collection chamber. When, what it is assumed to be plasma, enters this chamber the colour intensity drops below a certain limit (below 160 AU continuously for 20 s). When this condition is met a command, via Bluetooth, is sent to open the lower valve and so transfer the white blood cells to the second collection chamber.

4. Discussion

All the active valving methods previously described (in Sec. 1) are subjected to effects such as heating or piercing, not only at the valve position, but in an entire radial band as well because the actuation mechanism is activated during spinning. To overcome this limitation, other methods rely on stopping the disc and then aligning it with the actuator, which of course, results in a delay that might induce measurement errors in time-dependent assays. Furthermore, some systems are increased in complexity with the inclusion of XYZ

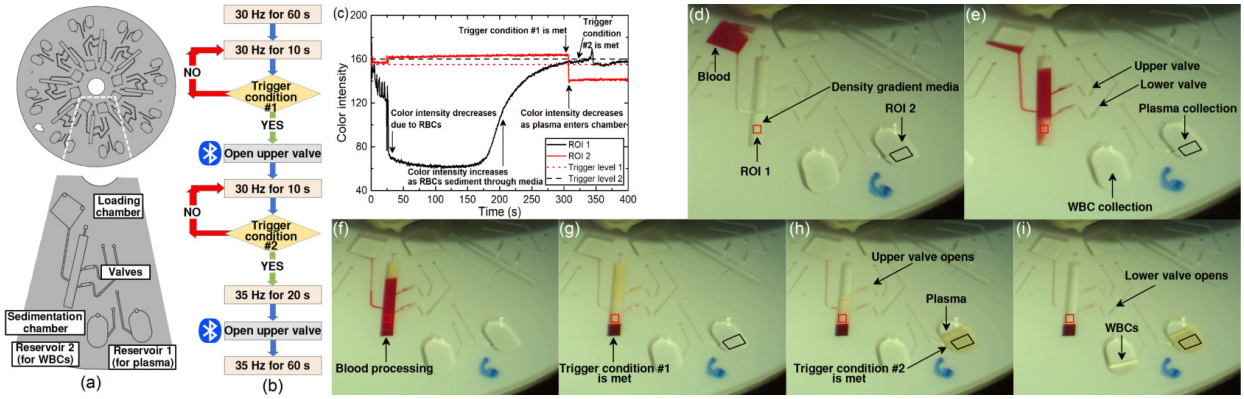

Figure 7: Closed-loop control of blood processing. (a) Schematic representation of the microfluidic disc used. (b) The program decision tree. Here, two triggers are used. Trigger Condition #1 is when the colour intensity in ROI 1 exceeds a cut off value (155 AU for 20 s unbroken) where this indicates that most red blood cells have sedimented through the density gradient media. Trigger Condition #2 is when the colour intensity drops below 160 AU (for 20 s unbroken) in ROI 2, this indicates the entry of plasma into the plasma collection chamber. (c) The motor spin-protocol and intensity plots for the entire experiment (See Movie-S5 available as supplementary material). Note that the colour of the intensity plots matches the ROIs shown in Fig. 7(d)-(i). Blood processing is indicated by a drop in colour intensity in ROI and its subsequent recovery. Entry of plasma into the plasma collection chamber is shown by a decrease in colour intensity in ROI 2. (d) Initialisation of blood processing (e-f) blood processing (g) blood processing is deemed completed as the colour intensity in ROI exceeds the cut-off value (h) upper valve opened to remove plasma (i) lower valve opened to remove white blood cells (WBCs in picture).

driving units. Here, we instead locally heated and melted a low-melting temperature membrane that vents a specific valve to atmosphere. Demonstrating in this way full integration and automation of on-disc active valving.

We believe that this approach could become an asset for time sensitive and highly multiplexed analytical assays due to the independence on the radial location of the valves and on the spinning frequency. Some assays that could take advantage of the qualities of this approach are Bradford assay (Redmile-Gordon et al., 2013) or an ELISA assay (Lee et al., 2009).

One of the well-known advantages of LOC systems, included LoaD among them, is the low volumes of sample and reagents required, which results in a significant decrease in their processing time. But the use of predefined, overtimed temporizers that make sure certain state has been reached increase the overall processing time. Instead, with closed-loop control, one can set the triggering signal for the release of reagents and samples immediately after the desired state has been accomplished. For instance, mixing in microfluidic systems is usually a challenge as, due to micro-scale effects, mass transport is typically via diffusion (relatively slow) rather than faster convection, hence the time to reach a certain degree of mixing is hard to predict. We demonstrated how through a closed-loop control certain mixing state (of reagent A and B, or sample and reagent) can be ensured and used to trigger a valve after a match of colour intensities is detected. While the work presented here relied on colour-based image analysis, the use of edge-detection can permit accurate on-disc volume measurements and analysis also of transparent liquids (Kazarine and Salin, 2014).

This approach allows also for higher tolerances in the analyte composition or variations in the environmental conditions, since the liquids are not automatically released after a fix time but as a result of the sedimentation state which is being indirectly monitored through the colour intensity measurement and therefore the centrifugation time is being automatically adjusted and presumably improving the reliability of the experiment.

Blood centrifugation, with follow-on plasma-based assays, is now ubiquitous in centrifugal microfluidics and indeed is one of the key advantages of the platform compared with non-centrifugal microfluidics. The use of closed-loop control, monitoring red blood cells, allowed us to stop the process in the minimal necessary time. This structure is demonstrated to show the potential of our approach to be integrated into common sample to answer centrifugation-based protocols which are commonly applied on the Lab-on-a-Disc. For example, our system of closed-loop control could, independently of our specific valving technology, be applied to work by Lee et al. (2009, 2011) and Cho et al. (2007) to perform plasma separation as part of immunoassays. Similarly, our monitoring technology could also be used in conjunction with work by Nwankire et al.

(2014) or Kinahan et al. (2016a) to implement multiplexed liver assay panels.

In our final experiment we showed a common and generic blood processing based procedure based on density gradient media to split the sample into its constituent red blood cells, plasma and white blood cells. However, we did not design this experiment for a specific assay, we rather conceived it as a generic tool from which many experiments could benefit, therefore, we stopped after this point. This experiment demonstrates how meaningful the closed loop flow-control is, as it requires two stage valving (an upper valve and a lower valve) which open in the correct sequence, requires we actuate the valves during rotation (to maintain the phase stability of plasma, white blood cells and the density gradient media), and the rate of red blood cells sedimentation is far slower through density gradient media than pure blood-based sedimentation. We have previously implemented and characterized density gradient media based blood processing in (Kinahan et al., 2016b).

In order to use our demonstrator as a real diagnostic device one would need to calibrate the arbitrary units from the image acquisition analysis because they now depend on the transparency of the materials used and the boundary conditions. Therefore, a further experiment is still needed to calibrate the trigger levels to correlate the colour intensity to the centrifugation level. For a given setup and material composition, these levels should then allow a reliable operation of the diagnostic system. The new system would allow to add precise in-situ measurements as trigger to the experiment instead of fix timed protocols that are based on previous experiments. Hence, this approach would be able to adapt to varying boundary condition as they might occur in real life and especially in point-of-care applications (Smith et al., 2016).

Although we limited ourselves to show only three exemplary experiments instead of one specific assay because we believe that the potential use of arbitrary and closed-loop controlled valving is vast and not bound to a specific case. The closed-loop control can also be applied to other triggering properties than colour. One could, for example, use temperature, pH, fluorescence or any other measurable quantity and thereby render broader the assays that can be achieve on disc.

5. Conclusions and outlook

In this paper we have introduced a novel valving mechanism for the centrifugal "Lab-on-a-Disc" platform by wireless control of rotor-based resistive heaters which locally melt temperature sensitive, on-disc membranes. The system has a response time of 3 s and enables actuation of an, until now, unprecedented number of valves. Significantly, the system is very light and obviates the need for physical connection; thus, it is compatible with very low-cost motors and could be integrated into portable systems. In addition, unlike many instrument actuated systems, the platform permits valve actuation during rotation. This makes it particularly suitable for applications that require accurate metering such as blood processing.

The main advantage from our platform over classic thermally induced phase change approaches is the level of integration that we achieved at an extremely low cost, size and power consumption. The capability for on-line closed-loop control of flow on the disc also offers great potential. Continuous monitoring can permit ‘on the fly’ optimization of systems and has the potential to identify issues and then intervene in real time, thereby drastically increasing the reliability of the result while potentially reducing the experiment time.

We envisage that this work sets the foundation for a new and ‘smarter’ generation of flow control on the centrifugal platform towards microfluidic large-scale integration (LSI). Therefore, we would like to encourage interested research groups to contact the group at the Karlsruhe Institute of Technology, to get an eLoaD platform so that you can explore the potential of the system for your own application.

Acknowledgements

This work was supported by the National Council of Science and Technology, CONACyT (Mexico), the University of Freiburg (Germany), the Karlsruhe Institute of Technology (Germany), the European Union (FP7-KBBE-2013-7-613908-DECATHLON and H2020-FETOPEN-1-2016-2017-737043-TISuMR) and by the Science Foundation Ireland (SFI) and Fraunhofer-Gesellschaft under the SFI Strategic Partnership Programme Grant Number 16/SPP/3321. The authors would like to acknowledge and thank Antoine Roland for manufacturing and assembling some of the discs used in this study. The authors are also thankful to Prof. Dr. Ulrike Wallrabe for providing access to her laboratories and measurement equipment at the University of Freiburg. We further acknowledge M.Sc. Fralett Suárez Sandoval for useful scientific discussions and Dr. Laura Weber for proofreading of the manuscript.

Appendix A. Supplementary material

Supplementary data associated with this article can be found in the online version at http://dx.doi.org/....

References

Abi-Samra, K., Hanson, R., Madou, M., Gorkin III, R.A., 2011. Infrared controlled waxes for liquid handling and storage on a cd-microfluidic platform. Lab Chip 11, 723–726.

Al-Faqheri, W., Ibrahim, F., Thio, T.H.G., Moebius, J., Joseph, K., Arof, H., Madou, M., 2013. Vacuum/compression valving (vcv) using parrafin-wax on a centrifugal microfluidic cd platform. PLoS One 8, 1–9.

Amasia, M., Cozzens, M., Madou, M.J., 2012. Centrifugal microfluidic platform for rapid {PCR} amplification using integrated thermoelectric heating and ice-valving. Sens. Actuators, B 161, 1191 – 1197.

Bartholomeusz, D.A., Boutté, R.W., Andrade, J.D., 2005. Xurography: rapid prototyping of microstructures using a cutting plotter. J. Microelectromech. Syst. 14, 1364–1374.

Burger, R., Kirby, D., Glynn, M., Nwankire, C., O'Sullivan, M., Siegrist, J., Kinahan, D., Aguirre, G., Kijanka, G., Gorkin, R.A., 2012. Centrifugal microfluidics for cell analysis. Curr. Opin. Chem. Biol. 16, 409–414.

Cai, Z., Xiang, J., Wang, W., 2015. A pinch-valve for centrifugal microfluidic platforms and its application in sequential valving operation and plasma extraction. Sens. Actuators, B 221, 257 – 264.

Carpentras, D., Kulinsky, L., Madou, M., 2015. A novel magnetic active valve for lab-on-cd technology. J. Microelectromech. Syst. 24, 1322–1330.

Chen, J.M., Huang, P.C., Lin, M.G., 2008. Analysis and experiment of capillary valves for microfluidics on a rotating disk. Microfluid. Nanofluid. 4, 427–437.

Cho, Y.K., Lee, J.G., Park, J.M., Lee, B.S., Lee, Y., Ko, C., 2007. One-step pathogen specific dna extraction from whole blood on a centrifugal microfluidic device. Lab Chip 7, 565–573.

Clime, L., Brassard, D., Geissler, M., Veres, T., 2015. Active pneumatic control of centrifugal microfluidic flows for lab-on-a-chip applications. Lab Chip 15, 2400–2411.

Czugala, M., Gorkin III, R., Phelan, T., Gaughran, J., Curto, V.F., Ducrée, J., Diamond, D., Benito-Lopez, F., 2012. Optical sensing system based on wireless paired emitter detector diode device and ionogels for lab-on-a-disc water quality analysis. Lab Chip 12, 5069–5078.

Ducrée, J., Haeberle, S., Lutz, S., Pausch, S., von Stetten, F., Zengerle, R., 2007. The centrifugal microfluidic bio-disk platform. J. Micromech. Microeng. 17, S103.

Höfflin, J., Torres Delgado, S.M., Suárez Sandoval, F., Korvink, J.G., Mager, D., 2015. Electrifying the disk: a modular rotating platform for wireless power and data transmission for lab on a disk application. Lab Chip 15, 2584–2587.

Garcia-Cordero, J.L., Kurzbuch, D., Benito-Lopez, F., Diamond, D., Lee, L.P., Ricco, A.J., 2010. Optically addressable single-use microfluidic valves by laser printer lithography. Lab Chip 10, 2680–2687.

Geissler, M., Clime, L., Hoa, X.D., Morton, K.J., HÃľbert, H., Poncelet, L., Mounier, M., DeschÃłnes, M., Gauthier, M.E., Huszczynski, G., Corneau, N., Blais, B.W., Veres, T., 2015. Microfluidic integration of a cloth-based hybridization array system (chas) for rapid, colorimetric detection of enterohemorrhagic escherichia coli (ehec) using an articulated, centrifugal platform. Anal. Chem. 87, 10565–10572. PMID: 26416260. http://dx.doi.org/10.1021/acs.analchem.5b03085.

Glynn, M., Kirby, D., Chung, D., Kinahan, D.J., Kijanka, G., Ducrée, J., 2013. Centrifugo-magnetophoretic purification of cd4+ cells from whole blood toward future hiv/aids point-of-care applications. J. Lab. Autom. 19, 285–296.

Glynn, M.T., Kinahan, D.J., Ducree, J., 2014. Rapid, low-cost and instrument-free cd4+ cell counting for hiv diagnostics in resource-poor settings. Lab Chip 14, 2844–2851.

Godino, N., Gorkin III, R., Linares, A.V., Burger, R., Ducrée, J., 2013. Comprehensive integration of homogeneous bioassays via centrifugo-pneumatic cascading. Lab Chip 13, 685–694.

Gorkin, R., Park, J., Siegrist, J., Amasia, M., Lee, B.S., Park, J.M., Kim, J., Kim, H., Madou, M., Cho, Y.K., 2010. Centrifugal microfluidics for biomedical applications. Lab Chip 10, 1758–1773.

Gorkin III, R., Clime, L., Madou, M., Kido, H., 2010. Pneumatic pumping in centrifugal microfluidic platforms. Microfluid. Nanofluid. 9, 541–549.

Gorkin III, R., Nwankire, C.E., Gaughran, J., Zhang, X., Donohoe, G.G., Rook, M., O'Kennedy, R., Ducrée, J., 2012. Centrifugo-pneumatic valving utilizing dissolvable films. Lab Chip 12, 2894–2902.

Grumann, M., Brenner, T., Beer, C., Zengerle, R., Ducrée, J., 2005a. Visualization of flow patterning in high-speed centrifugal microfluidics. Rev. Sci. Instrum. 76, 025101.

Grumann, M., Geipel, A., Riegger, L., Zengerle, R., Ducrée, J., 2005b. Batch-mode mixing on centrifugal microfluidic platforms. Lab Chip 5, 560–565.

Haeberle, S., Brenner, T., Zengerle, R., Ducrée, J., 2006. Centrifugal extraction of plasma from whole blood on a rotating disk. Lab Chip 6, 776–781.

Hwang, H., Kim, H.H., Cho, Y.K., 2011. Elastomeric membrane valves in a disc. Lab Chip 11, 1434–1436.

Hwang, H., Kim, Y., Cho, J., yoon Lee, J., Choi, M.S., Cho, Y.K., 2013. Lab-on-a-disc for simultaneous determination of nutrients in water. Anal. Chem. 85, 2954–2960. PMID: 23320485. http://dx.doi.org/10.1021/ac3036734.

Kawai, T., Naruishi, N., Nagai, H., Tanaka, Y., Hagihara, Y., Yoshida, Y., 2013. Rotatable reagent cartridge for high-performance microvalve system on a centrifugal microfluidic device. Anal. Chem. 85, 6587–6592.

Kazarine, A., Salin, E.D., 2014. Volumetric measurements by image segmentation on centrifugal microfluidic platforms in motion. Lab Chip 14, 3572–3581.

Kim, T.H., Sunkara, V., Park, J., Kim, C.J., Woo, H.K., Cho, Y.K., 2016. A lab-on-a-disc with reversible and thermally stable diaphragm valves. Lab Chip 16, 3741–3749.

Kinahan, D.J., Early, P.L., Vembadi, A., MacNamara, E., Kilcawley, N.A., Glennon, T., Diamond, D., Brabazon, D., Ducrée, J., 2016a. Xurography actuated valving for centrifugal flow control. Lab Chip 16, 3454–3459.

Kinahan, D.J., Kearney, S.M., Dimov, N., Glynn, M.T., Ducrée, J., 2014a. Event-triggered logical flow control for comprehensive process integration of multi-step assays on centrifugal microfluidic platforms. Lab Chip 14, 2249–2258.

Kinahan, D.J., Kearney, S.M., Faneuil, O.P., Glynn, M.T., Dimov, N., Ducrée, J., 2015. Paper imbibition for timing of multi-step liquid handling protocols on event-triggered centrifugal microfluidic lab-on-a-disc platforms. RSC Adv. 5, 1818–1826.

Kinahan, D.J., Kearney, S.M., Glynn, M.T., Ducrée, J., 2014b. Spira mirabilis enhanced whole blood processing in a lab-on-a-disk. Sens. Actuators, A 215, 71 – 76. Special Issue of the Micromechanics Section of Sensors and Actuators based upon contributions revised from the Technical Digest of the 26th {IEEE} International Conference on {MICRO} {ELECTRO} {MECHANICAL} {SYSTEMS} (MEMS-13; 20-24 January 2013, Taipei, Taiwan).

Kinahan, D.J., Kearney, S.M., Kilcawley, N.A., Early, P.L., Glynn, M.T., Ducrée, J., 2016b. Density-gradient mediated band extraction of leukocytes from whole blood using centrifugo-pneumatic siphon valving on centrifugal microfluidic discs. PLoS One 11, e0155545.

Kinahan, D.J., Renou, M., Kurzbuch, D., Kilcawley, N.A., Bailey, Ã., Glynn, M.T., McDonagh, C., Ducrée, J., 2016c. Baking powder actuated centrifugo-pneumatic valving for automation of multi-step bioassays. Micromachines 7, 175.

Kitsara, M., Nwankire, C.E., Walsh, L., Hughes, G., Somers, M., Kurzbuch, D., Zhang, X., Donohoe, G.G., O'Kennedy, R., Ducrée, J., 2014. Spin coating of hydrophilic polymeric films for enhanced centrifugal flow control by serial siphoning. Microfluid. Nanofluid. 16, 691–699.

Kong, M.C., Salin, E.D., 2012. Spectrophotometric determination of aqueous sulfide on a pneumatically enhanced centrifugal microfluidic platform. Anal. Chem. 84, 10038–10043.

Kong, M.C.R., Salin, E.D., 2010. Pneumatically pumping fluids radially inward on centrifugal microfluidic platforms in motion. Anal. Chem. 82, 8039–8041. PMID: 20815346. http://dx.doi.org/10.1021/ac102071b.

Lee, B.S., Lee, J.N., Park, J.M., Lee, J.G., Kim, S., Cho, Y.K., Ko, C., 2009. A fully automated immunoassay from whole blood on a disc. Lab Chip 9, 1548–1555.

Lee, B.S., Lee, Y.U., Kim, H.S., Kim, T.H., Park, J., Lee, J.G., Kim, J., Kim, H., Lee, W.G., Cho, Y.K., 2011. Fully integrated lab-on-a-disc for simultaneous analysis of biochemistry and immunoassay from whole blood. Lab Chip 11, 70–78.

Li, T., Zhang, L., Leung, K.M., Yang, J., 2010. Out-of-plane microvalves for whole blood separation on lab-on-a-cd. J. Micromech. Microeng. 20, 105024.

Loo, J., Kwok, H., Leung, C., Wu, S., Law, I., Cheung, Y., Cheung, Y., Chin, M., Kwan, P., Hui, M., Kong, S., Ho, H., 2017. Sample-to-answer on molecular diagnosis of bacterial infection using integrated lab-on-a-disc. Biosens. Bioelectron. 93, 212 – 219. Special Issue Selected papers from the 26th Anniversary World Congress on Biosensors (Part II).

Madou, M., Zoval, J., Jia, G., Kido, H., Kim, J., Kim, N., 2006. Lab on a CD. Annual review of biomedical engineering 8, 601–28.

Mark, D., Weber, P., Lutz, S., Focke, M., Zengerle, R., von Stetten, F., 2011. Aliquoting on the centrifugal microfluidic platform based on centrifugo-pneumatic valves. Microfluid. Nanofluid. 10, 1279–1288.

Miao, B., Peng, N., Li, L., Li, Z., Hu, F., Zhang, Z., Wang, C., 2015. Centrifugal microfluidic system for nucleic acid amplification and detection. Sensors 15, 27954–27968.

Mishra, R., Alam, R., Kinahan, D.J., Anderson, K., Ducrée, J., 2015. Lipophilic-membrane based routing for centrifugal automation of heterogeneous immunoassays, in: 2015 28th IEEE International Conference on Micro Electro Mechanical Systems (MEMS), pp. 523–526.

Moore, J.L., McCuiston, A., Mittendorf, I., Ottway, R., Johnson, R.D., 2011. Behavior of capillary valves in centrifugal microfluidic devices prepared by three-dimensional printing. Microfluid. Nanofluid. 10, 877–888.

Nwankire, C.E., Czugala, M., Burger, R., Fraser, K.J., Glennon, T., Onwuliri, B.E., Nduaguibe, I.E., Diamond, D., Ducrée, J., 2014. A portable centrifugal analyser for liver function screening. Biosens. Bioelectron. 56, 352–358.

Nwankire, C.E., Venkatanarayanan, A., Glennon, T., Keyes, T.E., Forster, R.J., DucrÃľe, J., 2015. Label-free impedance detection of cancer cells from whole blood on an integrated centrifugal microfluidic platform. Biosens. Bioelectron. 68, 382 – 389.

van Oordt, T., Barb, Y., Smetana, J., Zengerle, R., von Stetten, F., 2013. Miniature stick-packaging-an industrial technology for pre-storage and release of reagents in lab-on-a-chip systems. Lab Chip 13, 2888–2892.

Park, J.M., Cho, Y.K., Lee, B.S., Lee, J.G., Ko, C., 2007. Multifunctional microvalves control by optical illumination on nanoheaters and its application in centrifugal microfluidic devices. Lab Chip 7, 557–564.

Redmile-Gordon, M., Armenise, E., White, R., Hirsch, P., Goulding, K., 2013. A comparison of two colorimetric assays, based upon lowry and bradford techniques, to estimate total protein in soil extracts. Soil Biology and Biochemistry 67, 166 – 173.

Schwemmer, F., Zehnle, S., Mark, D., von Stetten, F., Zengerle, R., Paust, N., 2015. A microfluidic timer for timed valving and pumping in centrifugal microfluidics. Lab Chip 15, 1545–1553.

Siegrist, J., Gorkin, R., Clime, L., Roy, E., Peytavi, R., Kido, H., Bergeron, M., Veres, T., Madou, M., 2010. Serial siphon valving for centrifugal microfluidic platforms. Microfluid. Nanofluid. 9, 55–63.

Smith, S., Mager, D., Perebikovsky, A., Shamloo, E., Kinahan, D., Mishra, R., Torres Delgado, S.M., Kido, H., Saha, S., Ducrée, J., Madou, M., Land, K., Korvink, J., 2016. CD-Based Microfluidics for Primary Care in Extreme Point-of-Care Settings. Micromachines 7, 22.

Strohmeier, O., Keller, M., Schwemmer, F., Zehnle, S., Mark, D., von Stetten, F., Zengerle, R., Paust, N., 2015. Centrifugal microfluidic platforms: advanced unit operations and applications. Chem. Soc. Rev. 44, 6187–229.

Tang, M., Wang, G., Kong, S.K., Ho, H.P., 2016. A review of biomedical centrifugal microfluidic platforms. Micromachines 7.

Thio, T.H.G., Soroori, S., Ibrahim, F., Al-Faqheri, W., Soin, N., Kulinsky, L., Madou, M., 2013. Theoretical development and critical analysis of burst frequency equations for passive valves on centrifugal microfluidic platforms. Med. Biol. Eng. Comput. 51, 525–535.

Torres Delgado, S.M., Kinahan, D.J., Suárez Sandoval, F., Nirupa Julius, L.A., Kilcawley, N.A., Ducrée, J., Mager, D., 2016a. Fully automated chemiluminescence detection using an electrified-lab-on-a-disc (eload) platform. Lab Chip 16, 4002–4011.

Torres Delgado, S.M., Suárez Sandoval, F., Korvink, J.G., Mager, D., 2016b. A universal and stand-alone datalogger for lab-on-a-disc applications. 2016 IEEE, Proc. of Wireless Power Transfer Conference (WPTC) , 1–4.

Wang, G., Ho, H.P., Chen, Q., Yang, A.K.L., Kwok, H.C., Wu, S.Y., Kong, S.K., Kwan, Y.W., Zhang, X., 2013. A lab-in-a-droplet bioassay strategy for centrifugal microfluidics with density difference pumping, power to disc and bidirectional flow control. Lab Chip 13, 3698–3706.

WPC, 2016. Wpc qi specification version 1.2.2. https://www.wirelesspowerconsortium.com/downloads/download-wireless-power-specification.html. (accessed December 2017).

Zainal, M.A., Yunos, Y.M., Rahim, R.A., Ali, M.S.M., 2017. Wireless valving for centrifugal microfluidic disc. J. Microelectromech. Syst. PP, 1–8.
Zhu, Y., Chen, Y., Meng, X., Wang, J., Lu, Y., Xu, Y., Cheng, J., 2017. Comprehensive study of the flow control strategy in a wirelessly charged centrifugal microfluidic platform with two rotation axes. Anal. Chem. , null.